Mathematical Modelling of Circular plates with Combined Effects of Slip Velocity and surface Roughness on hydromagnetic Squeeze film

Jatinkumar. V. Adeshara[1], S. G. Sorathiya[2], Hardik P. Patel[3], G. M. Deheri[4] and R. M. Patel[5]

1. *Assistant Professor, Vishwakarma Government Engineering College, Chandkheda, Ahmedabad. - 382424 Gujarat State, India.*
2. *Assistant Professor, Department of Science, Sal Institute of Technology & Engineering research, Ahmedabad.*
3. *Department of Humanity and Science, L. J. Institute of Engineering and Technology Ahmedabad, Gujarat State India. .*
4. *Department of Mathematics, S. P. University, VallabhVidyanagar – 388 120, Gujarat State, India.*
5. *Department of Mathematics, Gujarat Arts and Science College, Ahmedabad - 380 006 Gujarat State, India.*

Abstract: *This paper discuss about the combined effect of transverse roughness and slip velocity on the performance of hydromagnetic fluid based rough rotated circular plates. The bearing surfaces are assumed to be transversely rough in nature. The results of slip velocity are adopted from Beavers and Joseph's slip model. To calculate the effect of transverse surface roughness has been employed to estimate the stochastic modeling of C&T. Reynolds' type equation is solved with appropriate boundary conditions to obtain the pressure Distribution in turn which leads to the calculation of load carrying Capacity. However, the negatively skewed roughness tends to enhance the performance of the bearing system. It is observed that the decreased load carrying capacity due to slip veIoci1y. It is noticed that the hydromagnetic fluid lubricant improves the performance of the bearing system. This investigation reveals that the negative effect of slip velocity and standard deviation associated with roughness can be compensated up to certain extent by the positive effect of hydromagnetic fluid in the case of negatively skewed roughness.*

Keywords: **Circular plates, hydromagnetization, longitudinal irregularaties, rotation, slip velocity**

Nomenclature:

r	Radial coordinate
a	Radius of the plate
$\dot{h}$	Velocity of S.F.
B_0	Uniform transverse magnetic field applied between the plates.
h_0	Initial film thickness
h	Lubricant's film thickness
s	Lubricant's Electrical conductivity
μ	Viscosity
M	$= B_0 h\left(\dfrac{s}{\mu}\right)^{1/2}$ = Hartmann number
h_0'	lower plate's surface width
h_1'	Upper plate's surface width
s_0	Electrical conductivity of lower surface
s_1	Electrical conductivity of upper surface
$\phi_0(h)$	$= \dfrac{s_0 h_0'}{sh}$ = Electrical permeability of the lower surface
$\phi_1(h)$	$= \dfrac{s_1 h_1'}{sh}$ = Electrical permeability of the upper surface
ρ	Density of lubricant

Ω_u	Upper plate's angular velocity
Ω_l	Lower plate's angular velocity
Ω_r	$\Omega_u - \Omega_l$
Ω_f	Ω_l / Ω_u – Rotation ratio
S	$= -\dfrac{h^3\rho\Omega_u{}^2}{\mu\dot{h}}$ = rotational inertia in non-dimensional form
p	Lubricant pressure
w	L.C.C.
σ^*	N.D. standard deviation (σ/h)
α^*	N.D. variance (α/h)
ε^*	N.D. skewness (ε/h^3)
P	N.D. pressure
W	Dimensionless L.C.C.
s	Slip Paramiter
s*	N.D. slip parameter

Abbreviation

L.C.C.	Load carrying Capacity
L.B.C.	Load bearing capacity
L.R.	L.R.
T.R,	T.R
M.F.	Magnetic field
B.C.	Boundary conditions
N.D.T.	Non-dimensional terms
N.D.	Non-dimensional
S.F.	Squeeze film

1. INTRODUCTION

In engineering science and industrial applications such as machine elements, gears, skeletal joints, bearings, bio-lubrication, and engine parts, discussions of squeezing film features play a key role. Typically, studies of S.F. activity reflect upon the structure lubricated with a non-conducting viscous liquid. In reality, if liquid metals such as mercury and sodium could be pumped or kept between the moving surfaces of the bearing, the application of a strong magnetic field could accommodate larger loads. The possibilities of electromagnetic pressurization from the application of an external magnetic field have been researched and studied because of the high electrical conductivity of liquid metals. Since liquid metals are good electrical conductors, the L.C.C. can be increased to allow use of the electromagnetic force. Overcoming the deficiency associated with high temperature lubricants and thereby relieving the low viscosity disadvantage.

Several experimental and theoretical research on plane metal bearing hydromagnetic lubrications have been discussed. Kuzma et.al. (1964) studied the behavior of magnetohydrodynamic S.F.s. The effect of plate conductivity on the efficiency of the bearing system has been investigated in this paper. It is shown that the bearing surfaces grow roughness after some run in and wear. Investigators studied the impact of irregularity C&T (1969a, 1969b, 1970). C&T (1969a, 1969b, 1970) Stochastic averaging method suggested a detailed general study for both L.R. and T.R. In a number of studies, Prajapati (1992), Gupta & Deheri (1996), Andharia et.al (1997), this method provided the basis for the study and review of the impact of surface irregularity.

Hydromagnetic S.F. properties have been explored for various geometries by Chou et. al. (2003), and Vadher et. al. (2008). Between spongy rotating rough circular plates, the magnetic fluid based S.F. was analyzed by Patel et. al. (2009). In Andharia, Deheri (2001, 2010, 2013), L.R. was studied in detail, Andharia et. al. (1999), Lin (2016) and Shimpi, Deheri (2016). Both of these research concluded that, in contrast with the case of T.R, L.R. had a less detrimental effect.

It was therefore advised to examine the impact of L.R. on hydromagnetic S.F. among rotating circular plates in the present research. The standard deviation related to L.R. plays an important role in this.

Shita. At.al. (2018) discussed magnetic fluid lubrication of a dual layered spongy S.F. in L.R. truncated conical plates considering slip velocity. Munsu.at.al (2019) states Influence of Ferrofluid Lubrication on L.R. Truncated Conical Plates with Slip Velocity.

2. ANALYSIS

Fig.-I displays the bearing system geometry and configuration. Although the upper plate travels along its normal toward the lower plate, the lower plate is assumed rotating. The plates are electrically conductive and an electrically conductive lubricant fills the clearance gap in between. Between the two plates, a uniform transverse magnetic field is applied.

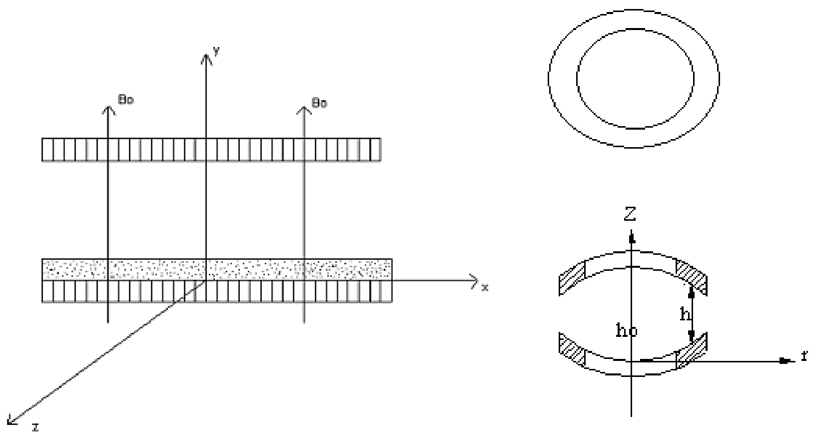

Figure. – I Geometry of the bearing system

The surfaces of bearing are taken to be transversely rough. The film thickness is brought from C&T (1969a, 1969b, 1970).

The film of the lubricant is isoviscous, incompressible and the flow is normally laminar. The updated Reynolds equation describing the lubricant film pressure is obtained as, according to the normal assumptions of hydromagnetic lubrication (Prajapati (1995), Bhat (2003)).

$$\frac{1}{r}\frac{\partial}{\partial r}\left[r\frac{\partial p}{\partial r}\right]=\frac{\mu\dot{h}}{AB}+2\rho\left(\frac{3}{10}\Omega_r^2+\Omega_r\Omega_l+\Omega_l^2\right) \tag{1}$$

where

$$A=\left[\frac{2}{M^3}\left[\frac{M}{2}-\tanh\frac{M}{2}\right]\right], \qquad B=\left[\frac{\phi_0+\phi_1+1}{\phi_0+\phi_1+\left(\tanh\frac{M}{2}\right)/\left(\frac{M}{2}\right)}\right]$$

As a consequence, conventional hydromagnetic lubrication hypotheses and follow-up discussions of Vadher et al., (2008), Andharia & Deheri (2013), C & T (1969a, 1969b, 1970), and Patel et. al. (2009), One comes to the stochastically averaged Reynolds form equation concerned, resorting to the irregularity (longitudinal) formula as a model of irregularity (longitudinal).

$$\frac{1}{r}\frac{\partial}{\partial r}\left[r\frac{\partial p}{\partial r}\right]=\frac{\mu\dot{h}}{m(h)\,AB}+2\rho\left(\frac{3}{10}\Omega_r^2+\Omega_r\Omega_l+\Omega_l^2\right) \tag{2}$$

where

$$m(h)=[(h^3+3h^2\alpha+3h(\alpha^2+\sigma^2)+\varepsilon+3\sigma^2\alpha+\alpha^3)]*\left((1+4s\bar{h})/1+2s\bar{h})\right)$$

With the use of Reynolds' B.C.

p = 0 when r = a

and

$$\frac{\partial p}{\partial r}=0 \text{ at } r=0 \tag{3}$$

Now integrating equation (2) and applying B.C. (3), one gets the S.F. pressure Dist. in the form of

$$p=\left(\frac{\mu\dot{h}}{m(h)\,AB}+2\rho\left(\frac{3}{10}\Omega_r^2+\Omega_r\Omega_l+\Omega_l^2\right)\right)\left(\frac{r^2-a^2}{4}\right) \tag{4}$$

Using the following N.D.T. in equation (4)

$$R=\frac{r}{a},\ \sigma^*=\frac{\sigma}{h},\ \alpha^*=\frac{\alpha}{h},\ \varepsilon^*=\frac{\varepsilon}{h^3},\ S=-\frac{h^3\rho\Omega_u{}^2}{\mu\dot{h}},\ s^*=s\bar{h}$$

one derives the Dist. of pressure in dimensionless as

$$P=-\frac{ph^3}{\mu\dot{h}\pi a^2}=\left(\frac{1}{M(h)AB}-\frac{S}{5}\left(3\Omega_f^2+4\Omega_f+3\right)\right)\frac{(1-R^2)}{4\pi} \tag{5}$$

Where

$$M(h)=(1+3\alpha^*+3(\alpha^{*2}+\sigma^{*2})+\varepsilon^*+3\sigma^{*2}\alpha^*+\alpha^{*3})*((1+4s^*)/1+2s^*))$$

In fact, the load is the internal pressure originated between the opposite surfaces due to the dynamic action. The L.B.C. given by

$$w=2\pi\int_0^a p(r)\cdot r\,dr,$$

is computed in dimensionless form as

$$W = -\frac{wh^3}{\mu \dot{h} \pi a^4}$$

$$= \frac{1}{8\pi}\left(\frac{1}{M(h)AB} - \frac{S}{5}\left(3\Omega_f^2 + 4\Omega_f + 3\right)\right) \tag{6}$$

3. RESULTS AND DISCUSSIONS

It is easily seen from equations (4) and (6) that the Dist. of pressure and the load depend on different quantities such as M, $\phi_0+\phi_1$, σ^*, ε^*, α^*, S ,Ω_f and s*. Setting the values of σ^*, α^*, ε^*, S, Ω_f and s* to be zero the present study diminishes to study of Shukla,Prasad (1965) for a smooth non– spongy, irrotating conducting plate while in limiting case taking $M \rightarrow 0$ this study trim down to the analysis of Prakash,Vij (1973) for non–magnetic case. The outcomes of Patel-Gupta (1979) are found when electrical permeability of both the surfaces are considered to be zero.

It is clearly seen that as hydromagnetization parameter and electrical permeability of both the surfaces increases, the LBC increases for a fixed values of σ^*, α^*, ε^*, S, Ω_f and s*. The effect of conductivity on the profile of pressure and Dist. of LBC originates from the factor

$$\frac{(\phi_0 + \phi_1) + \left(\tanh\frac{M}{2}\right)\left(\frac{M}{2}\right)^{-1}}{(\phi_0 + \phi_1) + 1}$$

This factor tends to

$$\frac{(\phi_0 + \phi_1)}{(\phi_0 + \phi_1) + 1}$$

for bigger values of M as $\tanh(M/2) \rightarrow 0$. These function are increasing functions of $\phi_0+\phi_1$ and from the mathematical terms one can see that as $\phi_0+\phi_1$ increses, the pressure and LCC increase as well.

A closed look at these Fig.s (1) to (7) depicts that the load W increases marginally with regards to the magnetization parameter M. Further, (-ve) skewed irregularitiess helps to improve the bearing behaviour, same as with (-ve) variance. It is appealing to note that the increasing in load induced by (-ve) variance is sharper and the (+) variance in general, has a (-ve) effect on the system.

From Fig.s (8) to (13) it is clearly observed that the L.C.C.increases significantly w.r.t $\phi_0+\phi_1$. The standard deviation associated with T.R. helps in decreasing the L.B.C. which is unlikely in the case of L.R.. (Fig.s (14) to (18)).

Fig.s (19) to (25) establish that the negatively skewed irregularities enhances the load as in the case of variance (– ve). These trends reverse for positively skewed irregularities and variance (+ ve). The profile of L.C.C. of rotational inertia w.r.t rotation ratio and slip parameter is presented in Fig. (26) and (27). A maximum value of load is observed when the plates rotates in opposite directions. The profile of L.C.C is in fig (28) increases in rotational ratio w.r.t slip parameter.

From these Fig.s one can conclude that the opposing effect induced by variance positive, positive skewness and rotational inertia can be neutrilized up to certain extent in the case of skewness(-ve), espacially when the negative variance is involved. In general, the bearing suffers due to roughness. Given analysis offers plenty scopes for enhancing the bearing performance in the case of (-ve) skewed roughness, espacially when variance (–ve) is considered and this positive effect is further enriched by the combined effect of combined electrical permeability of bearing surfaces and parameter of magnetization(M).

Using these results alone mentions that the machine's life period can be extended in the case of T.R. bearing systems. This analysis also makes it clear that the T.R parameters must given due consideration while designing the such type of bearing systems, even if the suitable choice of M and $\phi_0+\phi_1$ has been taken into account.

4. CONCLUSION

This article proposes that the slip parameter must be kept at a minimum for an overall improved bearing system efficiency. Therefore, this research demonstrates that the irregularities aspect must be carefully considered when designing the bearing system. This study appears to show that in the case of negative skewed roughness, the adverse effect of slip velocity can be substantially reduced by hydromagnetic lubrication as the standard deviation associated with irregularities causes decreased load. As compared to the case of L.R patterns, it is noted that the condition remains relatively better even though slip velocity is involved. In spite of the fact that there are numerous constraints causing load reduction, this type of bearing system supports a good amount of load even in the absenteeism of flow, which fails to happen in the case of conventional lubricant, based bearing system.

REFERENCES

[1]. Andharia, P. I. and Deheri, G. M., Effect of longitudinal surface roughness on the behavior of S.F. in a spherical bearing, International Journal of Applied Mechanics and Engineering, 6(4), **(2001)**, p.p. 885-897.

[2]. Andharia, P. I. and Deheri, G. M., L.R. effect on magnetic fluid based S.F. between conical plates, Industrial Lubrication and Tribology, 62(5), **(2010)**, p.p. 285-291.

[3]. Andharia, P. I. and Deheri, G. M., Performance of magnetic fluid based S.F. between longitudinally rough elliptical plates, ISRN Tribology, Article ID482604, (2013) 6 pages.

[4]. Andharia, P. I., and Gupta, J. L. and deheri, G. M., Effect of longitudinal surface roughness on hydrodynamic lubrication of a slider bearings. In proceding of The Tenth International Conference on surface modification Technologies. **(1997)**, p.p. 872-880.

[5]. Andharia, P. I., and Gupta, J. L. and deheri, G. M., Effect of transverse surface roughness on the behaviour of S.F. in spherical bearing. Journal of Applied Mechanical Engineering, 4, **(1999)**, p.p. 19-24.

[6]. Bhat, M. V., Lubrication with a magnetic fluid, Team Spirit, India, Pvt. Ltd. **(2003)**.

[7]. Chou, T. L., Lai, J. W. and Lin, J. R., Magneto-hydrodynamic S.F. characteristics between a sphere and a plane surface, Journal of Marine Science and Technology, 11(3), **(2003)**,p.p. 174-178.

[8]. Christensen, H. and Tonder, K. C. Tribology of rough surfaces: stochastic models of hydrodynamic lubrication. SINTEF, Report No. 10/69. **(1969a)**, p.p. 18

[9]. Christensen, H. and Tonder, K. C., Tribology of rough surfaces: parametric study and comparison of lubrication models. SINTEF, Report no 22/69. **(1969b)**,P.p. 18

[10]. Christensen, H. and Tonder, K. C., Tribology of rough surfaces: a stochastic model of mixed lubrication. SINTEF, Report no. 18/70. **(1970)**, p.p. 21.

[11]. Gupta, J. L. and Deheri, G. M. Effect of roughness on the behaviour of S.F. in a spherical bearing. Tribology Tranjection. 39. **(1996)**, P.p.99-102.

[12]. Kuzma, D. C., Maki, E. M.and Donnelly, R. J., The magnehydrodynamic S.F.s. Journal of Fluid Mechanic, 19, **(1964)**, p.p. 395-400.

[13]. Lin, J. R., Longitudinal surface roughness effects in magnetic fluid lubricated journal bearing, Journal of Marine Science and Technology, 24(4), **(2016)**, p.p. 711-716.

[14]. M Munsu, A Patil, G Daher., Influence of Ferrofluid Lubrication on Longitudinally Rough Truncated Conical Plates with Slip Velocity., Mathematical Journal of Interdisciplinary Sciences., Vol. 7(2), **(2019)**, p.p.93–101.,

[15]. Patel, H., Deheri G. M. and Patel R. M., , Magnetic Fluid based S.F. between porous rotating rough circular plates, Industrial Lubrication and Tribology, 61(3), **(2009)**, p.p. 140-145.

[16]. Patel, K. C. and Gupta, J. L. Behaviour of hydromagnetic S.F. bewtween porous plates.Wear, 56. **(1979)**, p.p. 327-339.

[17]. Patel, H., Deheri G. M. and Patel R. M., Magnetic Fluid based S.F. between porous rotating rough circular plates, Industrial Lubrication and Tribology, 61(3), **(2009)**, p.p. 140-145.

[18]. Prajapati, B. L. S.F. behaviour between rotating porousn circular plates with concentric circular pocket: surface roughness and elastic deformation effects. Wear, 152. **(1992)**, p.p. 301-307.

[19]. Prakash, J. and Vij, S. K. L.C.C. and time height relation for S.F. between porous plates. Wear, 24. **(1973)**, p.p. 309-332.

[20]. Shimpi, M. E. and Deheri, G. M., , Combine effect of bearing deformation and L.R. on the performance of a ferrofluid based S.F. together with velocity slip in truncated conical plates, Imperial journal of Interdisciplinary research, 2(8), **(2016),** p.p. 1423-1430.

[21]. Shita A Patel, A Patil, G Daher., Magnetic Fluid Lubrication Of A Double Layered Porous S.F. In Longitudinally Rough Truncated Conical Plates Considering Slip Velocity. Journal of Emerging Technologies and Innovative Research Vol. 5(7). **(2018)**, P.p. 330-335.

[22]. Vadher, P. A., Vinodkumar, P. C., Deheri, G. M. and Patel, R. M., Behavior of hydromagnetic S.F.s between two conducting rough porous circular plates, Journal of Engineering Tribology, Vol. 222(4), **(2008)**,p.p.659-679.

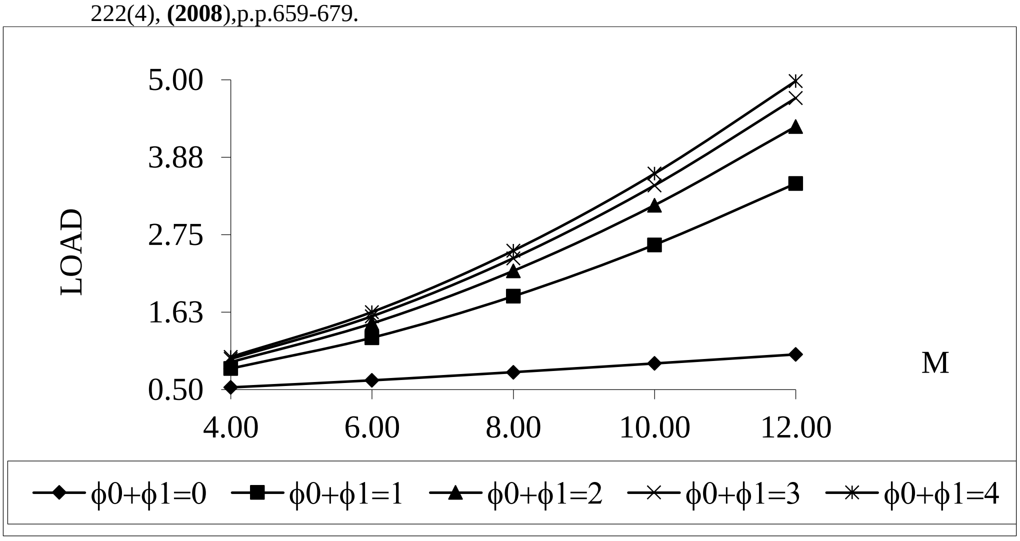

Figure: 1 Variation of load carrying capacity with respect to M and $\phi_0+\phi_1$

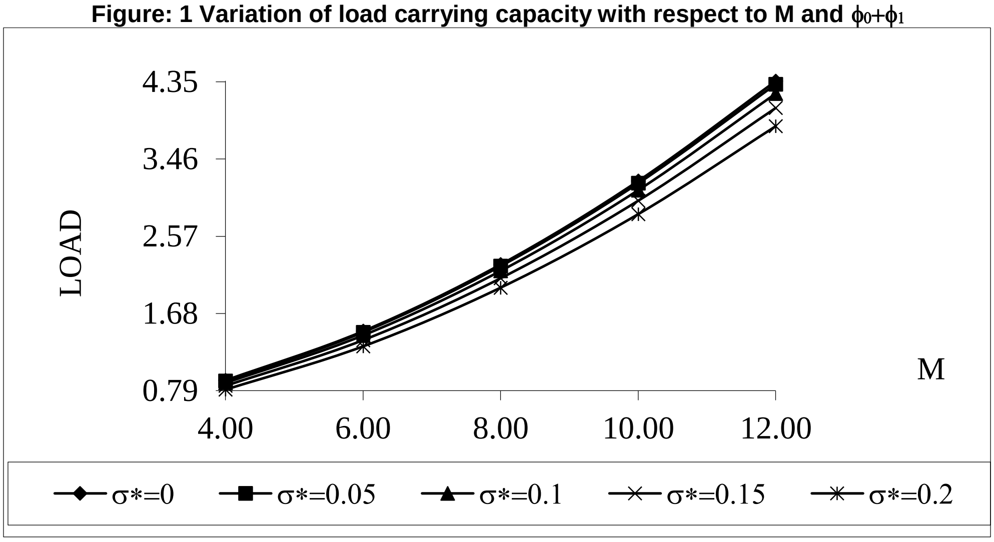

Figure: 2 Distribution of load for M and $\sigma*$

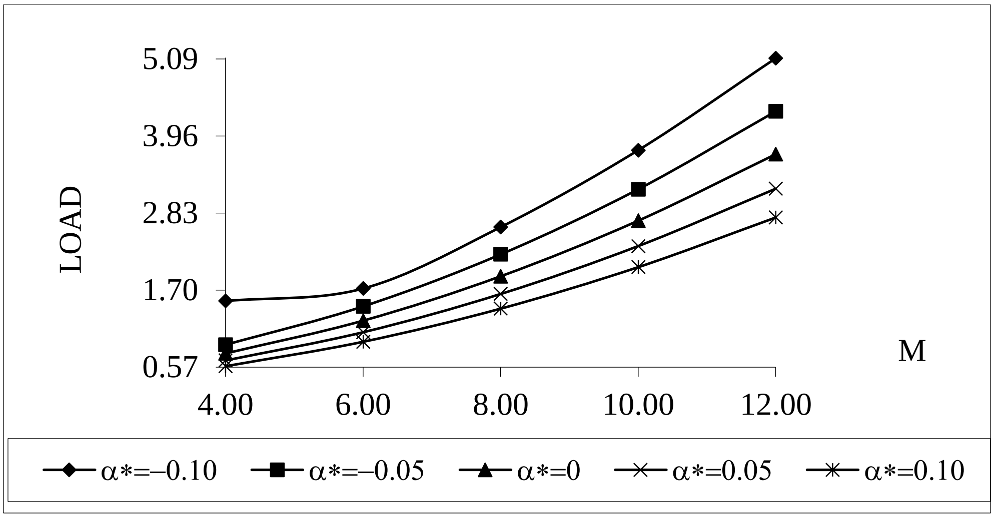

Figure: 3 Profile of load bearing capacity with regards to M and α*

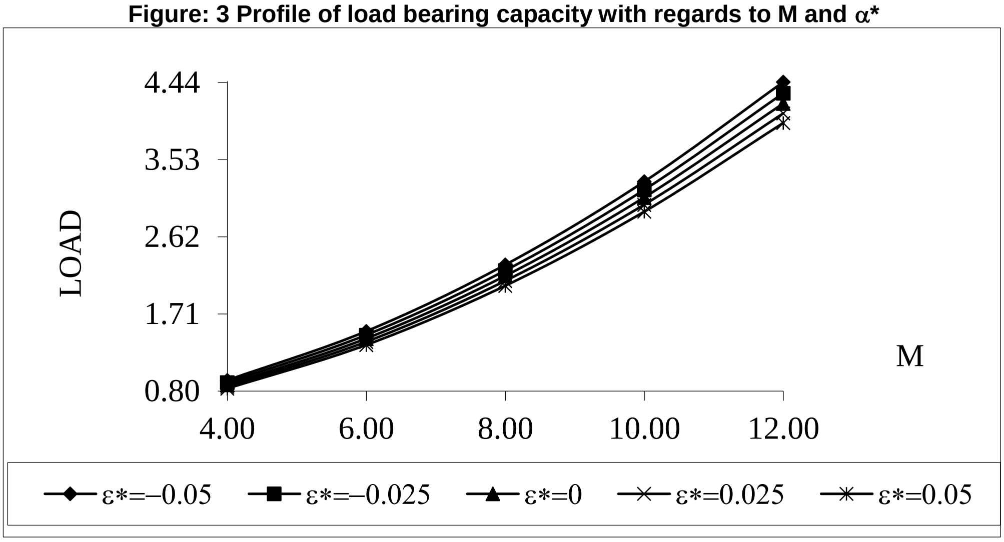

Figure: 4 Variation of load carrying capacity with respect to M and ε*

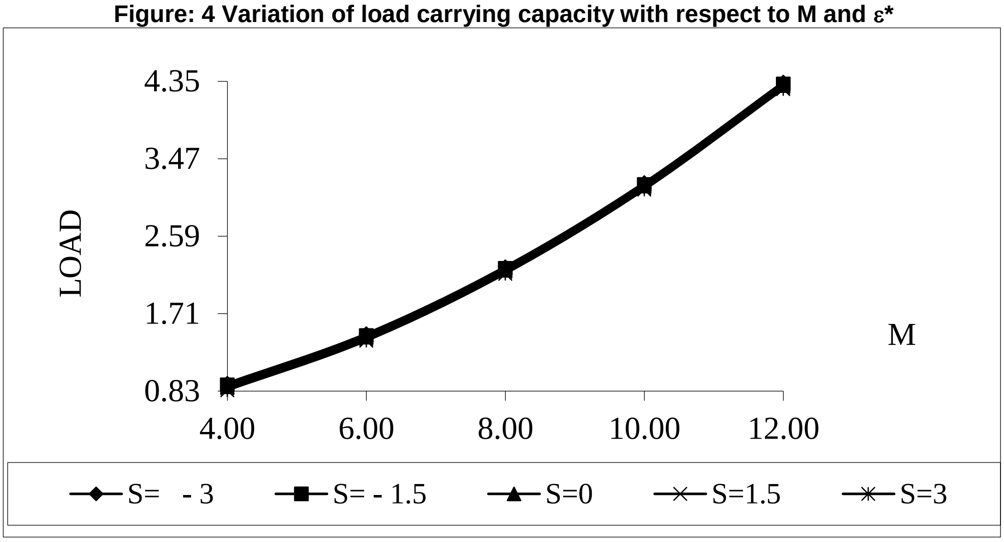

Figure: 5 Distribution of load for M and S

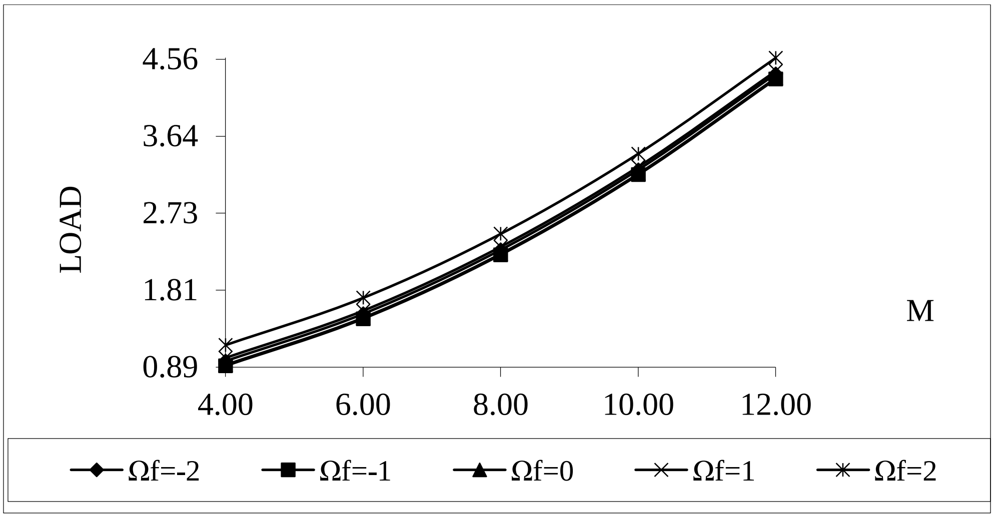

Figure: 6 Profile of load bearing capacity with regards to M and Ω_f

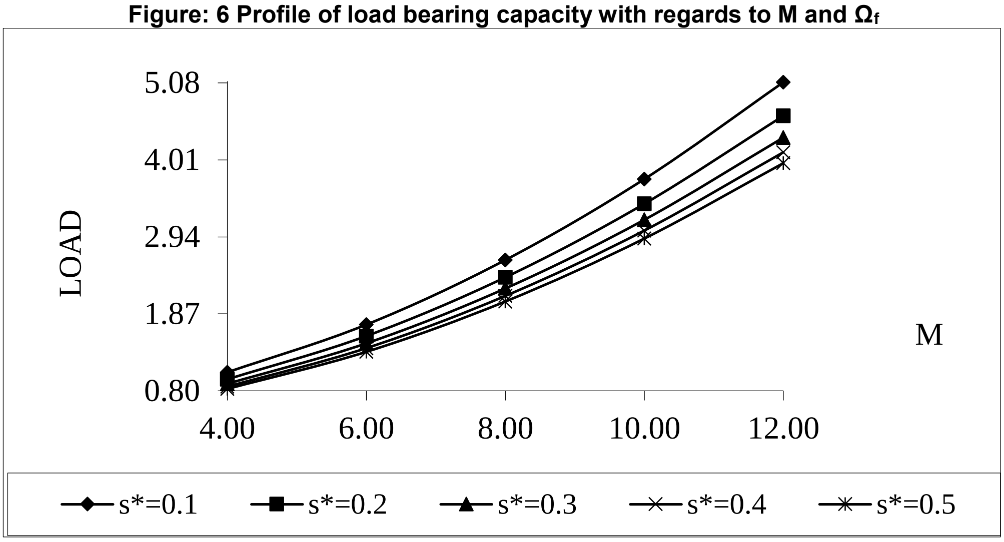

Figure: 7 Profile of load bearing capacity with regards to M and s*

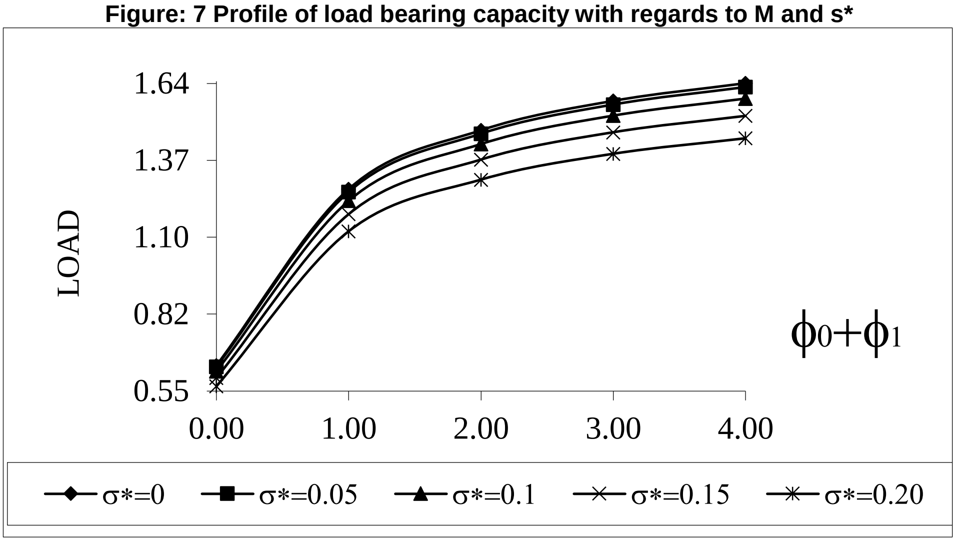

Figure: 8 Variation of load carrying capacity with respect to $\phi_0+\phi_1$ and σ*

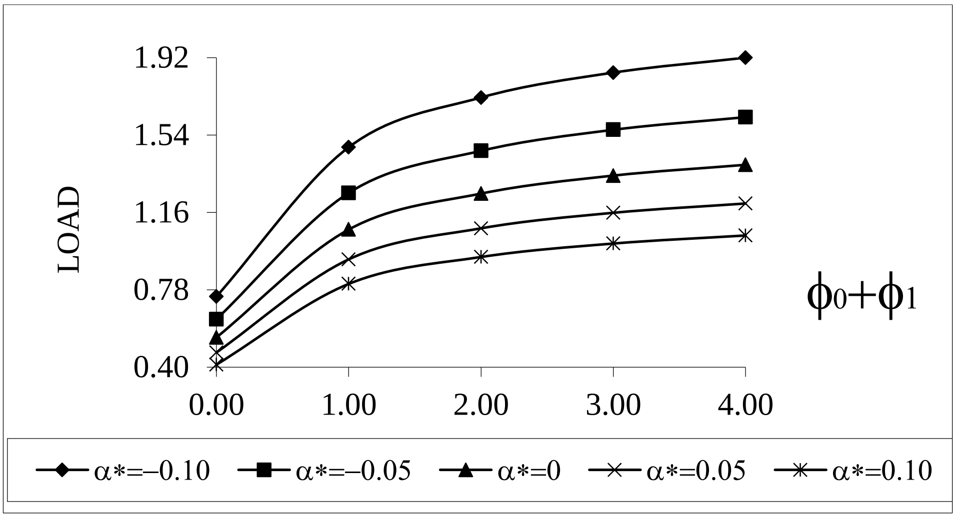

Figure: 9 Distribution of load for $\phi_0+\phi_1$ and α^*

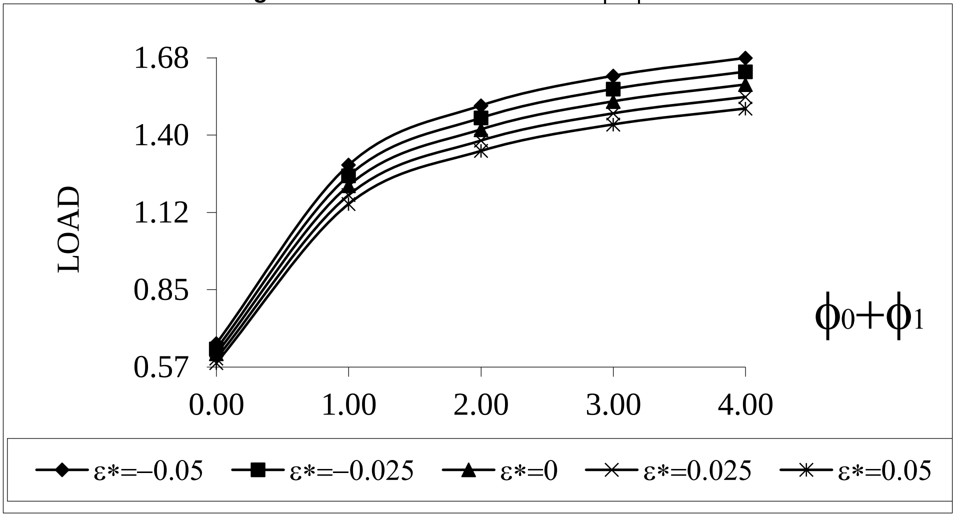

Figure:10 Profile of load bearing capacity with regards to $\phi_0+\phi_1$ and ε^*

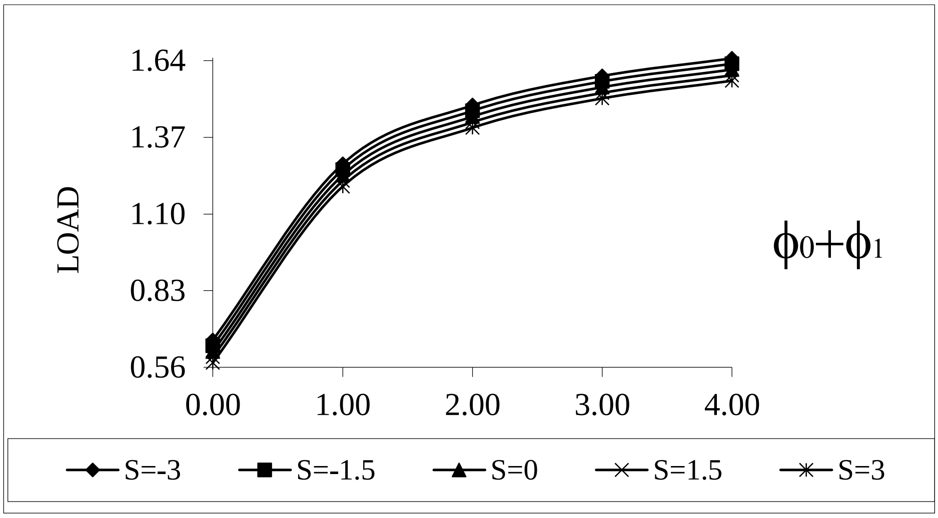

Figure: 11 Variation of load carrying capacity with respect to $\phi_0+\phi_1$ and S

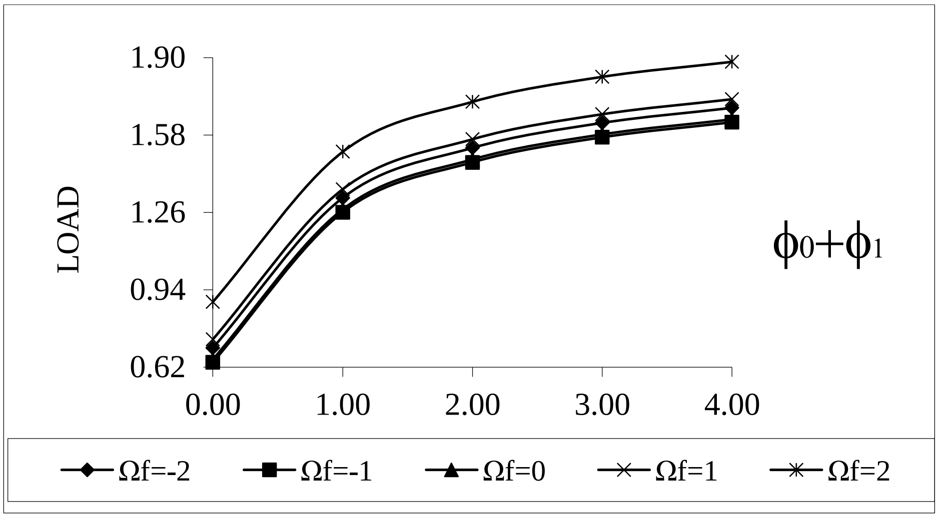

Figure: 12 Distribution of load for $\phi_0+\phi_1$ and Ω_f

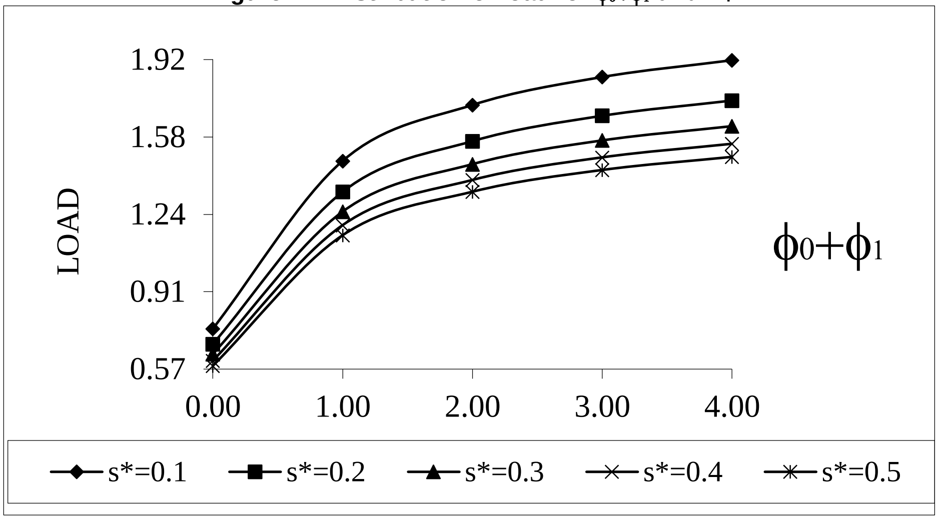

Figure: 13 Distribution of load for $\phi_0+\phi_1$ and s*

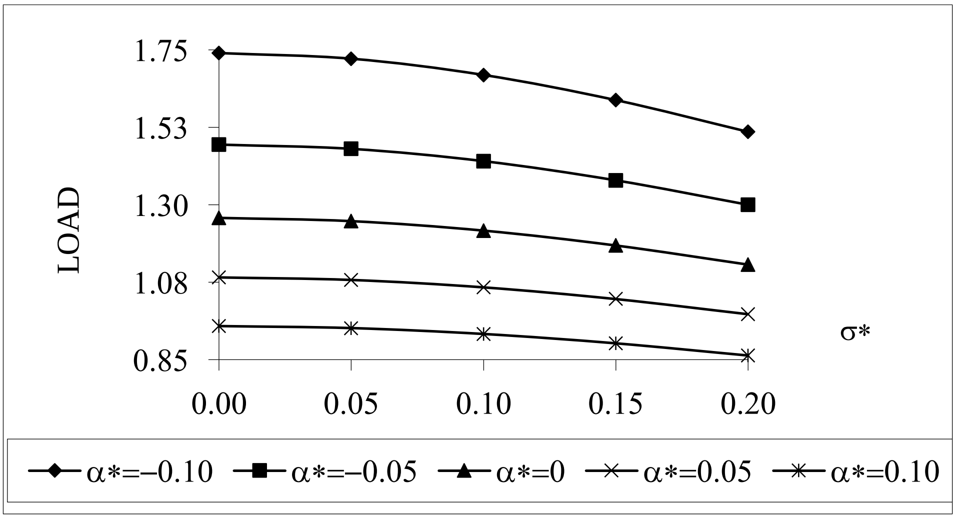

Figure: 14 Profile of load bearing capacity with regards to σ^* and α^*

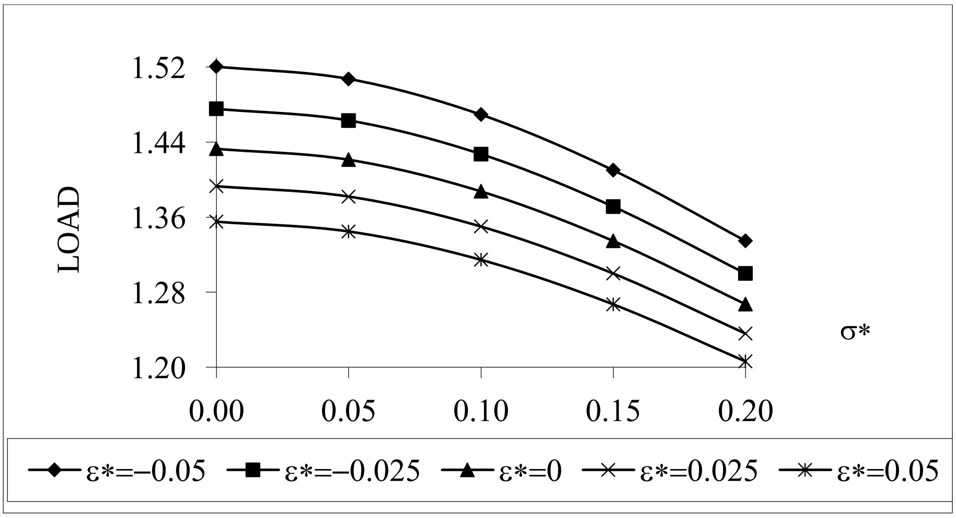

Figure: 15 Variation of load carrying capacity with respect to σ* and ε*

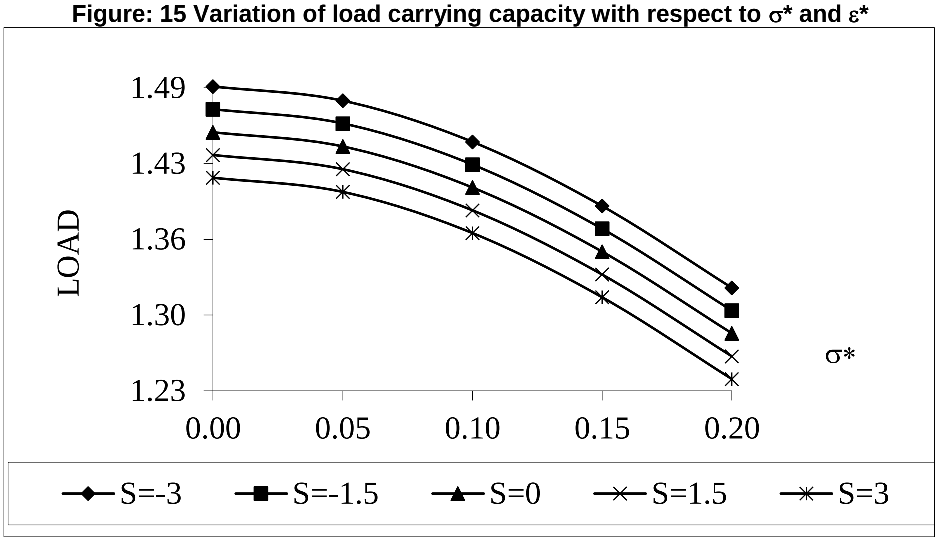

Figure: 16 Distribution of load for σ* and S

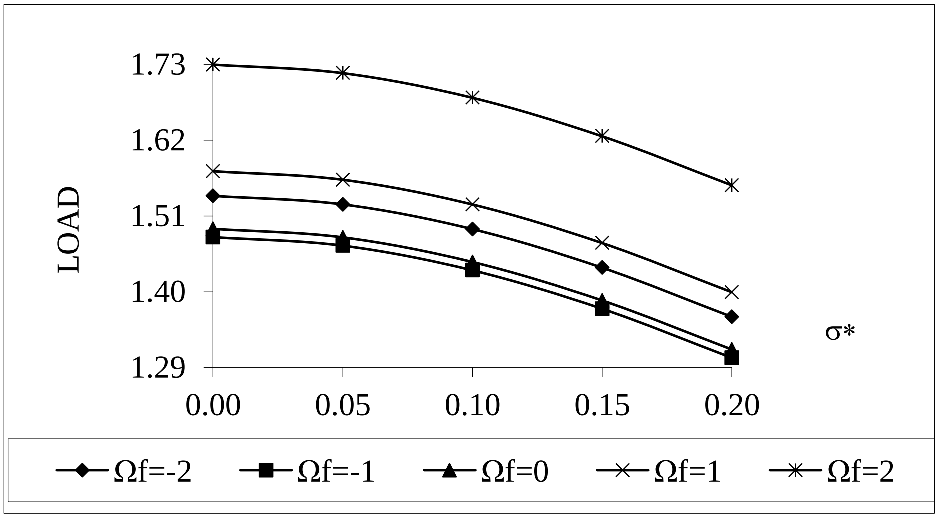

Figure: 17 Profile of load bearing capacity with regards to σ* and Ω_f

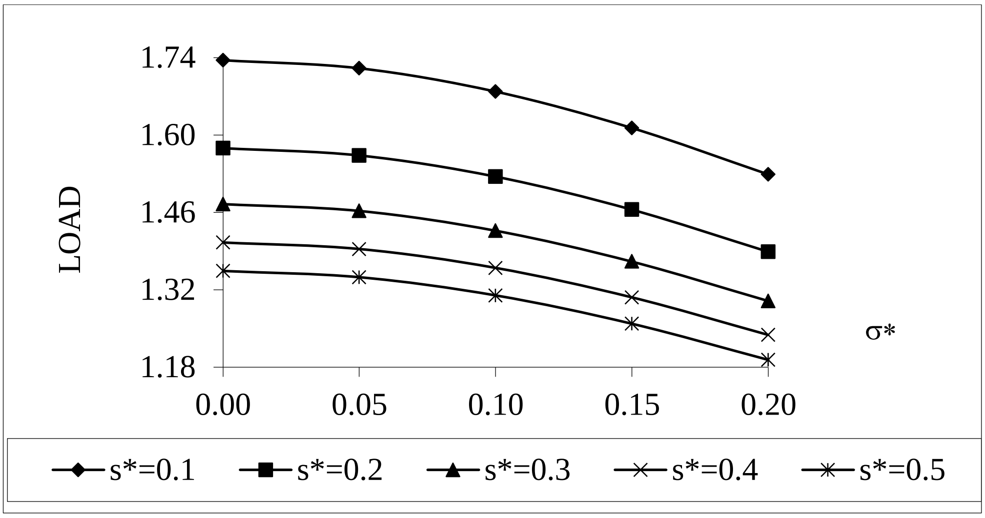

Figure: 18 Profile of load bearing capacity with regards to σ* and s*

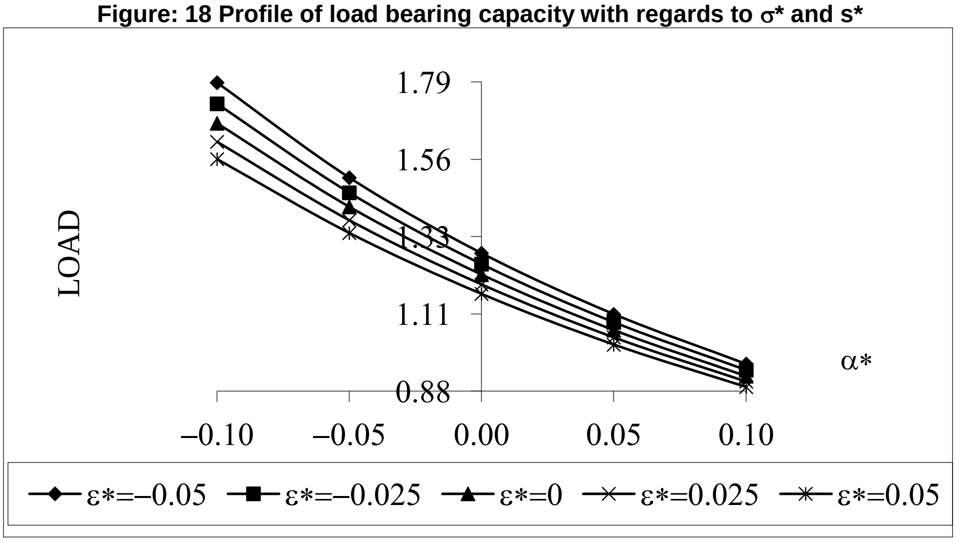

Figure: 19 Variation of load carrying capacity with respect to α* and ε*

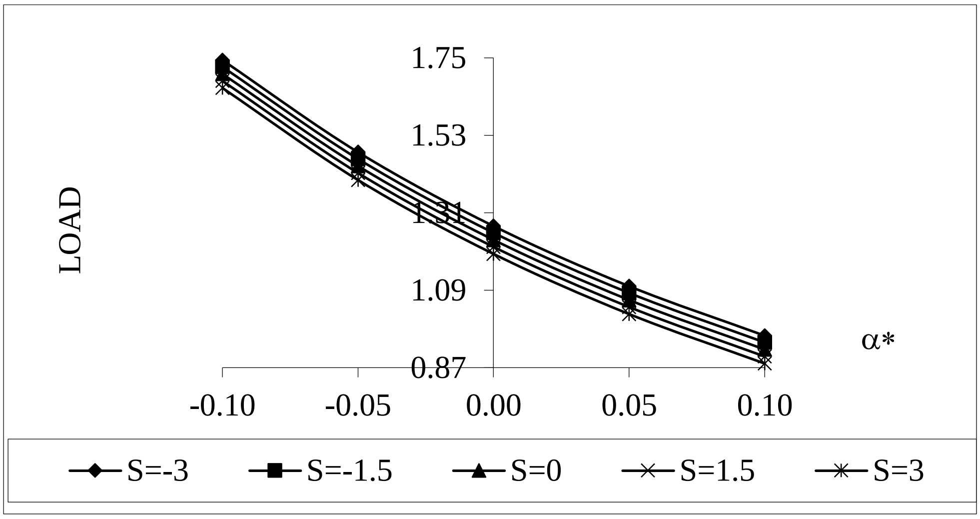

Figure: 20 Distribution of load for α* and S

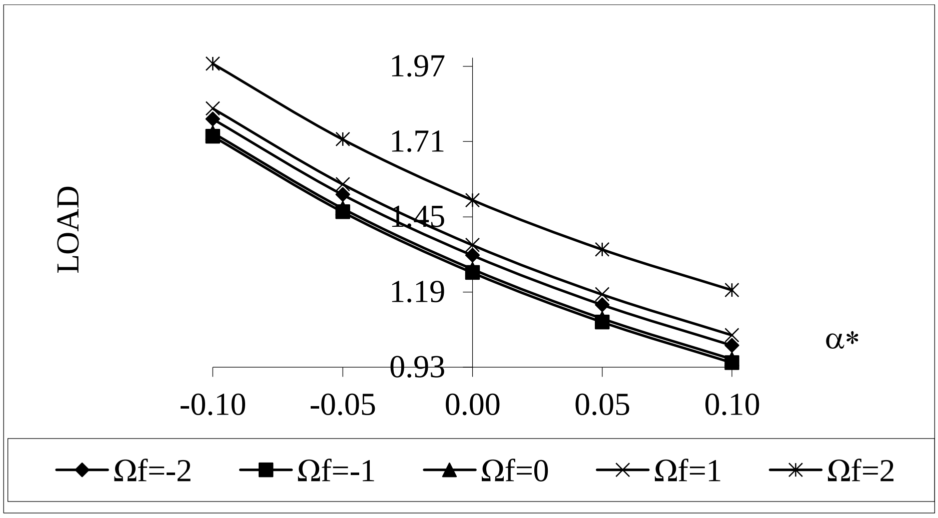

Figure: 21 Profile of load bearing capacity with regards to α* and Ω_f

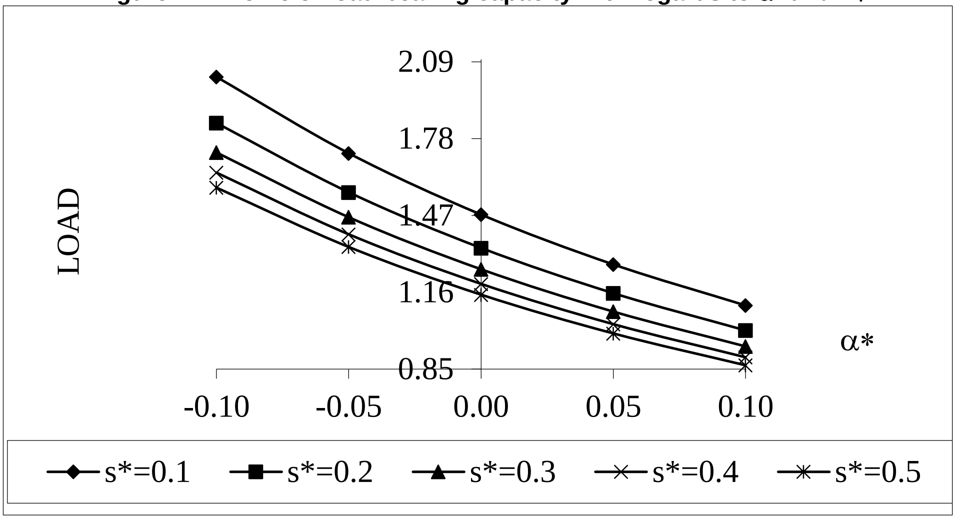

Figure: 22 Profile of load bearing capacity with regards to α* and s*

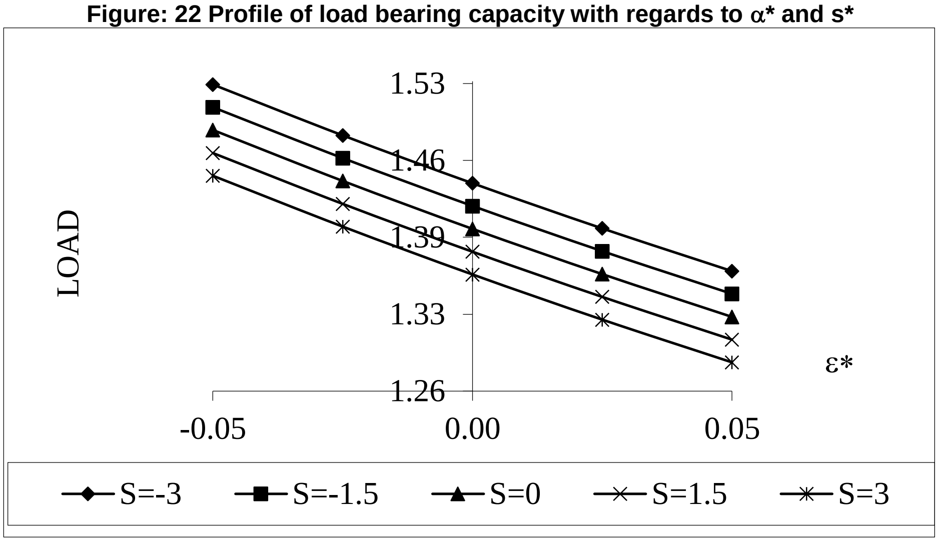

Figure: 23 Variation of load carrying capacity with respect to ε* and S

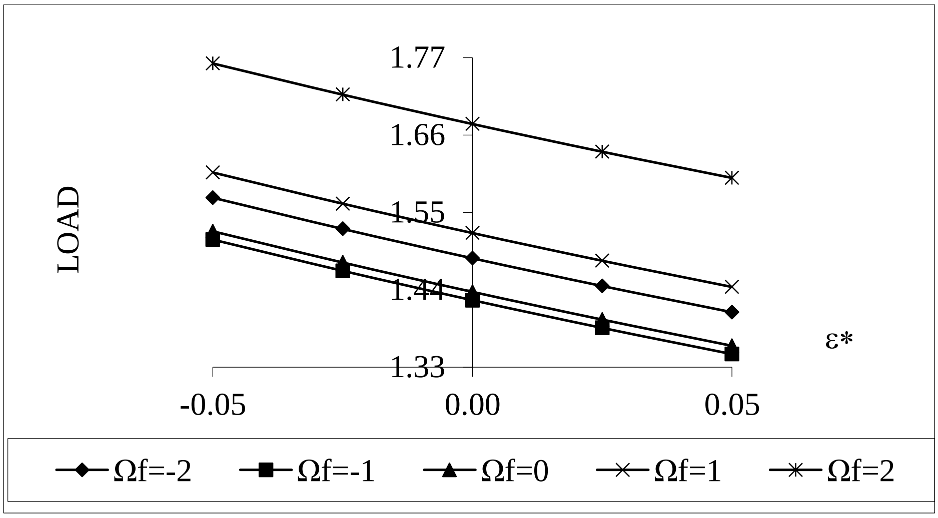

Figure: 24 Distribution of load for ε* and Ω_f

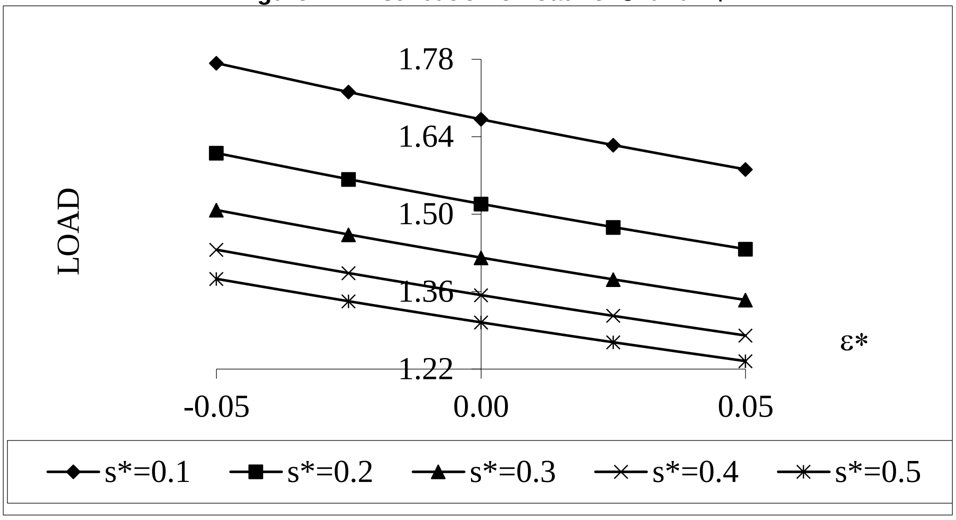

Figure: 25 Distribution of load for ε* and s*

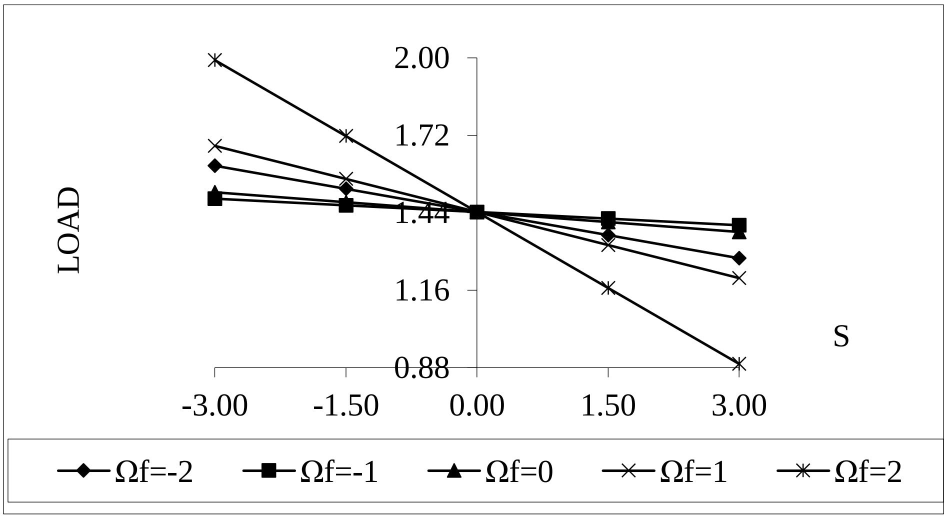

Figure: 26 Profile of load bearing capacity with regards to S and Ω_f

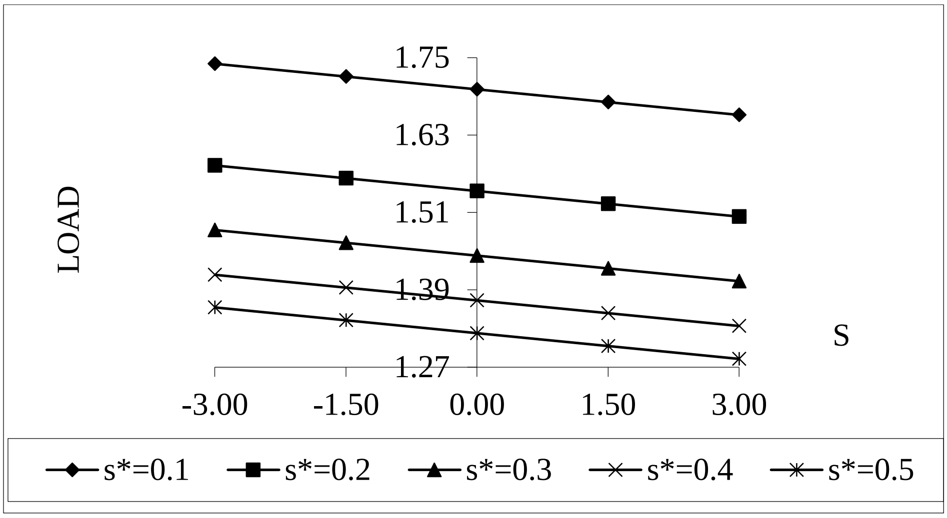

Figure: 27 Profile of load bearing capacity with regards to S and s*

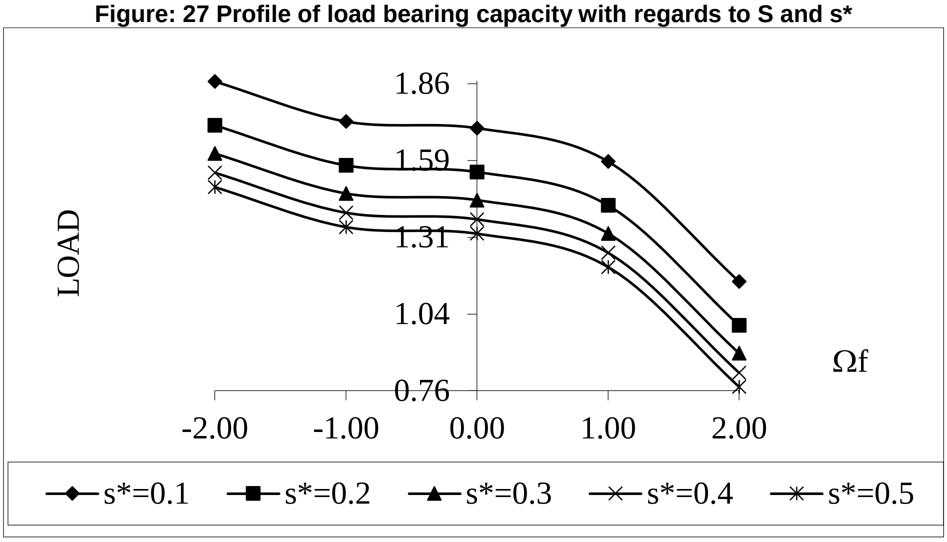

Figure: 28 Profile of load bearing capacity with regards to Ω_f and s*